INL/JOU--18-50161
Accepted Manuscript

Thermodynamic Stability Studies of Ce-Sb Compounds with Fe

Yi Xe, Jinsou Zhang, Michael T. Benson, Robet D. Mariani

February, 2018

The INL is a
U.S. Department of Energy
National Laboratory
operated by
Battelle Energy Alliance

Prepared for the U.S. Department of Energy
Office of Nuclear Energy
Under DOE Idaho Operations Office
Contract DE-AC07-05ID14517

Thermodynamic Stability Studies of Ce-Sb Compounds with Fe

Yi Xie[a], Jinsuo Zhang[a]*, Michael T. Benson[b], Robert D. Mariani[b]

a. Nuclear Engineering Program, Mechanical Engineering Department, Virginia Tech, Blacksburg, VA 24061, U.S.

b. Idaho National Laboratory, P.O. Box 1625, MS 6188, Idaho Falls, ID 83415, U.S.

*Corresponding author, Email: zjinsuo5@vt.edu, Phone: (540) 231-1198, Postal address: 635 Prices Fork Rd, Blacksburg, VA 24061, U.S.

Abstract

Lanthanide fission products can migrate to the fuel periphery and react with cladding, causing fuel-cladding chemical interaction (FCCI). Adding a fuel additive dopant, such as Sb, can bind lanthanide, such as Ce, into metallic compounds and thus prevent migration. The present study focuses on the thermodynamic stability of Ce-Sb compounds when in contact with the major cladding constituent Fe by conducting diffusion couple tests. Ce-Sb compounds have shown high thermodynamic stability as they did not react with Fe. When Fe-Sb compounds contacted with Ce, Sb was separated out of Fe-Sb compounds and formed the more stable Ce-Sb compounds.

Keywords: Fuel additive Sb; Diffusion couple test; Ce-Sb compounds; Fe-Sb compounds; FCCI

1. Introduction

Metallic nuclear fuels, such as U-Zr with HT-9 cladding (a ferritic martensitic steel), have been extensively studied and recognized as the fuel candidate for sodium-cooled fast reactors. However, the application of U-Zr fuel is limited by cladding degradation caused by fuel-cladding chemical interaction (FCCI) [1] [2]. FCCI formation in metallic fuel is strongly dependent on temperature and the temperature-gradient present across the fuel, which provides a driving force for diffusion and migration of constituents to the fuel/cladding interface [3]. Lanthanide (Ln) fission products, such as Ce, are known to be the key elements leading to FCCI. In post-irradiation fuels, significant lanthanide precipitates have been found at the outer region of fuel and the cladding layers [4]. Lanthanide precipitates at the fuel periphery have been found at even low burnups, indicating the migration is rapid [5]. With enough interdiffusion, the concentration ratio of lanthanide to the major cladding constituents, such as Fe, will increase, causing intermetallic compounds to precipitate, which tend to be brittle or have low melting temperatures.

Recent studies on lanthanide immobilization have found that adding fuel additives, such as Sb [6], Pd [7], Sn [8] and In [9], can effectively bind lanthanide to intermetallic compounds. These compounds can immobilize lanthanide in the fuel, and thus improve the chemical stability and mitigate FCCI. In U-Zr-Sb alloys, precipitates of Sb and a fraction of Zr were observed [6]. In U-Zr-Sb-Ce alloys, which were casted by adding the appropriate amount of Ce to the pre-alloy of U-Zr-Sb, the release of Zr from the Sb-Zr precipitates to make Ce-Sb intermetallic compounds strongly suggested the effectiveness of Sb in its action to bind lanthanide fission products as they are produced [6]. The intermetallic compounds observed were Ce_4Sb_3 and Ce_2Sb, with excess Sb dissolved in the fuel matrix and not depleting Zr from the fuel matrix [6]. In U-Zr-Pd-Ln alloys, Pd collocated with Ln in the ratio of 1:1 at most regions [7]. Similarly, in U-Zr-Sn-Ln alloys, Sn

collocated with Ln in the forms of Ln_5Sn_3 and possibly $(Ln,Zr)_5Sn_3$ [8]. Indium (In) displayed similar behaviors to Pd and Sn [9]. However, Pd, Sn and In did not fully release Zr back into the fuel matrix like Sb did, instead, they consumed a fraction of Zr and formed Pd/Sn/In-Zr-Ln precipitations in the alloys. It has not been determined if these intermetallics have dissolved Zr, or if Zr is part of the intermetallics, forming a ternary compound. Either way, the Zr content is lessened in the fuel matrix, lowering the fuel solidus temperature. Among these candidate additive dopants, Sb appears to show high binding preference for lanthanide while effectively releasing Zr into the fuel matrix.

Although the previous study indicated that Ce will bind Sb over other fuel constituents, it is possible that some Ce, produced during irradiation, and Ce-Sb compounds, will come in contact with the fuel cladding. In either case, it is important to know what interactions are likely to occur, i.e., will Ce-Sb compounds react with Fe, and if Ce-Fe compounds form, can that be reversed if Sb becomes available? Therefore, understanding the stability of Ce-Sb compounds when in contact with Fe, the major constituent of cladding, is needed. There are two ways to address these questions. The first is to assess the thermodynamic properties of the Ce-Sb-Fe system, and the second is to compare the thermodynamic stability between the Ce-Sb and Fe-Sb systems. The phase diagram and the thermodynamic properties of the Ce-Sb-Fe system can indicate the formation of ternary compounds and the formation enthalpy. However, available data are very limited. Current knowledge is still constrained to the binary systems, including the Ce-Sb [10] and Fe-Sb [11] systems. There are four known intermetallic compounds (Ce_2Sb, Ce_4Sb_3, CeSb and $CeSb_2$) in the Ce-Sb system [10], and one intermediate compound $Fe_{1.27}Sb$ and one intermetallic compound $FeSb_2$ in the Fe-Sb system [11]. Based on the enthalpy of formation, there is a greater driving force to form Ce-Sb compounds compared to Fe-Sb compounds [12] [13]. However, simply comparing the enthalpy of formation cannot support the stability of Ce-Sb compounds. Experimental results are needed to compare the spontaneity of forming Ce-Sb, Fe-Sb, or ternary Ce-Sb-Fe compounds as well as to qualitatively evaluate the stability of Ce-Sb compounds.

The present work aims to study the stability of Ce-Sb compounds when in contact with Fe. The simplified system selected makes it possible to fully understand the interactions between Ce-Sb compounds and Fe; however, using the real cladding materials, such as HT-9, should be conducted in the future to determine if interactions will occur between Ce-Sb compounds and the other constituents present in the cladding. Previous experimental studies on the isothermal diffusion couple consisting of U-23Zr-1Ce at.% fuel alloy and Fe did not find Ce-rich phases at the interface, possibly because of the effect of the U-Zr rind and the short reaction time [14]. To eliminate the possible influence of U-Zr rind on the fuel casting and to focus on the reactions of Ce-Sb compounds and Fe, the present work used pure Ce and Sb metals as test materials instead of U-Zr-Sb-Ce alloys. This experimental setup presents the worst case scenario, similar to the actual lanthanide fission products pressed directly on the cladding as a consequence of lanthanide migration and fuel swelling. The work does not aim to yield rate data, accordingly, only a single temperature and single time were presented.

According to the recognized thermodynamic properties [12] [13] [15], it's anticipated that the chemical interactions between Ce and Fe with Sb addition become less active than without Sb addition. The diffusion couple method is one of the experimental techniques frequently used in the phase diagram determination [16], and this method was used in our assessment of intermetallic compound formation. Combined with the scanning electron microscopy (SEM) analysis, the

metallic phases and elemental distribution at the Ce/Fe interface with and without the addition of Sb have been analyzed and compared.

2. Materials and Experiment

Four diffusion couple tests were performed by: 1) joining two plane-parallel discs of Ce and Fe, 2) joining the two (Ce and Fe) discs with an extremely thin layer of Sb powder in between, 3) joining the Sb-diffused Ce disc obtained in test 2 with a new Fe disc, and 4) joining the Sb-diffused Fe disc obtained in test 2 with a new Ce disc. The Ce and Fe discs were 20 mm × 20 mm × 2 mm with 99.9 % purity obtained from ESPI Metals, and the Sb powder was 200-mesh with 99.999 % purity obtained from Alfa Aesar. The Ce discs were shipped in an argon-filled container. All the samples were opened in the argon-filled glovebox, where oxygen level < 0.1 ppm and moisture level < 2 ppm. The bounding surface was rubbed on a clean napped polishing pad to fully remove oxides, which is similar with the process in Ref. [17]. Note that the polishing process that running with water and diamond paste were not applied in this work, as water would rapidly oxidize cerium.

The test surfaces were coupled, the couple was then wrapped with Ta foil to prevent reactions with other materials, and then clamped in a Kovar alloy. The fixture is shown schematically in Figure 1. Kovar alloy was used as it has a low heat expansion. The clamped couple was isothermally heat-treated at 853 K for 72 h in the furnace in the glovebox. After the heat-treatment, the couple was taken out of furnace and placed in Si-based quenching oil (in glovebox) for 1 minute to preserve the high-temperature phase equilibrium. The post-test sample was stored in the glovebox. SEM analysis was conducted within 24 h after test to mitigate the effects of oxidation.

The test temperature was selected for the following reasons. Firstly, 853 K was selected because the typical temperatures of the sodium-cooled fast reactor cladding are at 693–913 K [7]. Secondly, 853 K is below the eutectic melting temperatures of Ce-Fe, Ce-Sb and Fe-Sb systems. If the temperature was above the eutectic melting temperatures, it would make a melt structure at the Ce/Fe interface to flow around the couple. At a temperature below the eutectic melting temperature, the effects can be less dramatic yet diffusion-based interaction can be observed.

Although the test environment contained extremely low oxygen, the Ce disc was visibly tarnished after heat-treatment. Therefore, the diffusion couple center, which was tightly clamped and less affected by oxygen, was prepared for analysis. The interdiffusion interface was cut perpendicularly to reveal the reaction zones, and then mounted, grinded and polished to 1 μm in air. The final polish was completed in less than 2 minutes to reduce the effects of rapid oxidation, after that, the sample was placed in the SEM immediately for analysis. The SEM instrument (model: FEI Quanta 600 FEG) was equipped with a Bruker energy dispersive spectrometer (EDS) and silicon drift detector (SDD). The EDS was controlled by Esprit 1.9 software for image acquisition and micro-analysis. The SEM was operated at an accelerating voltage of 20 kV and spot size 5. EDS spectra were collected over the energy range 0-10 keV. EDS resolution was 1 μm at the 20 kV accelerating voltage.

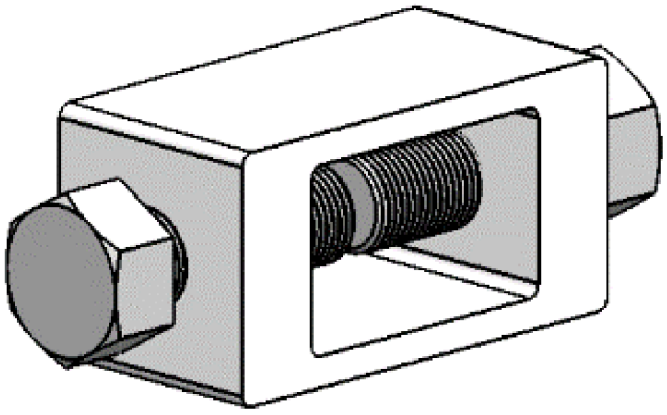

Figure 1 Schematic diagram of the Kovar alloy fixture. The diffusion couple was clamped between the two bolts.

3. Results and Discussion

3.1 Ce-Fe diffusion couple

The Ce-Fe diffusion couple was isothermally heat-treated at 853 K for 72 h, and the cross section of the interdiffusion layers is shown in the top of Figure 2. The black phase on the right of the SEM image is pure Fe. The grey region next to Fe is the Ce-Fe interdiffusion layer. Based on the EDS data (points 1-3 in Table 1), the layer contains about 32-33 at.% Ce and 67-68 at.% Fe, which corresponds to the intermetallic compound $CeFe_2$. The light grey region (labeled with "Ce-Fe diffusion" in Figure 2) next to the $CeFe_2$ layer is comprised of 17-22 at.% Fe (points 4-6, Table 1), with the remainder being Ce. This is an Fe-diffusion region, with intermetallics not formed or too small to detect. The left half in Figure 2 is Ce, with a small amount of Fe (e.g. at a distance ~100 μm in the EDS line). After heat-treatment, Ce became very brittle. The diffusion of Fe in the Ce substrate accounts for the brittleness and the contamination from polishing. The elemental profiles corresponding to the scan line in Figure 2 shows that the $CeFe_2$ layer is about 150 μm, and the Ce-Fe diffusion layer is about 450 μm.

A previous Ce-Fe diffusion couple test at 698 K for 96 h found the $CeFe_2$ layer to be 22 μm [18], the difference should be caused by temperature, which is the major factor influencing the diffusion and reaction kinetics. At a higher temperature, the diffusion and reaction regions are larger, and Fe has a larger diffusion kinetics to diffuse into the Ce substrate. This also explains the existence of Ce-Fe diffusion layer in the present work, while was not present in the previous study at 698 K [18]. With a long enough time of diffusion couple test, the location of the Ce-Fe diffusion layer as shown in Figure 2 would consist of $CeFe_2$ compound if enough Fe was diffused into this area.

In this diffusion couple, diffusion only occurred in one direction, from the Fe side into the Ce. This was also observed in a previous diffusion couple [19]. This is not the case during irradiation, though, as a recent post-irradiation examination of U-10Zr shows [20]. Figure 13 in Ref. [20] clearly shows lanthanide diffusion into the cladding, as well as Fe diffusion into the fuel. This difference between irradiation and out-of-pile testing is likely caused by the temperature gradient present during irradiation, with the hot zone in the center of the fuel. Although this difference exists, it should not impact the information gained from the current investigation. The purpose of

this study is to investigate the stability of Ce-Sb compounds when in contact with Fe. This can be accomplished in out-of-pile testing without temperature gradients.

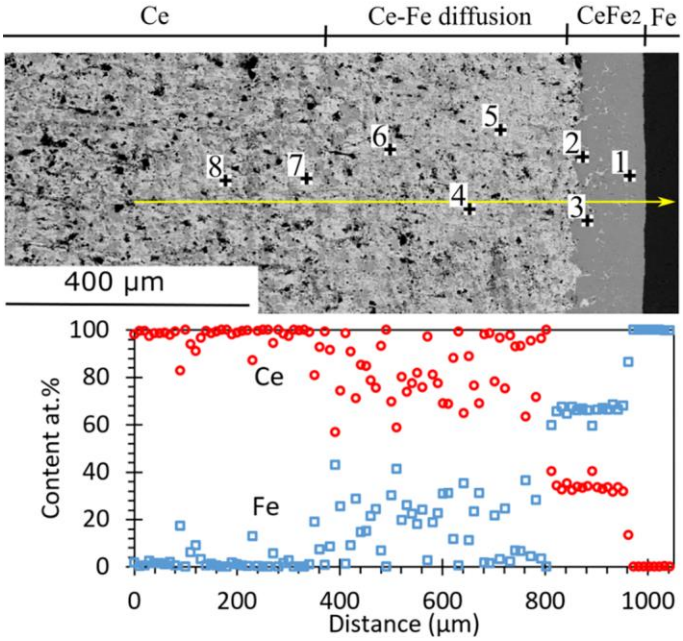

Figure 2. SEM backscattered electron (BSE) image for the cross section of Ce- Fe diffusion couple (top) and elemental profile corresponding to the scan line (bottom). EDS data are listed in Table 1.

Table 1. EDS data for points shown in Figure 2 (at.%).

	Fe	Ce
1	67.33	32.67
2	67.91	32.09
3	67.84	32.16
4	18.75	81.25
5	17.92	82.08
6	22.43	77.57
7	0.00	100.00
8	0.00	100.00

3.2 Ce-Sb-Fe diffusion couple

A thin layer of Sb powder was evenly deposited on the Ce-Fe bounding surfaces and heated at 853 K for 72 h. Unlike the Ce-Fe diffusion couple discussed in Section 3.1, with the addition of Sb, Ce and Fe did not interdiffuse; rather, the discs were separated after the test. Visibly, the Sb powder was firmly adhered on the Ce and Fe metal surfaces. Binary phases of Ce-Sb and Fe-Sb are likely causing the adhesion. The process of using a powder interface in a diffusion couple has been used to establish equilibria phases between diffusion couple materials [21] (in this case between Ce and

Fe). Compared with a solid Sb foil or disc, the Sb porous powder can accelerate the diffusion process. It has been found that the more rapid intermetallic layer growth in porous powder than in solid diffusion couples [22]. Since the present work aims to study the intermetallic compounds formed among Ce, Sb and Fe, and evaluate their thermodynamic stability, the results should not be affected by the physical form.

The Ce and Fe discs were separately sectioned and mounted for SEM analysis. The cross section SEM images are shown in the top of Figure 3. In the left SEM image, from left to right the phases are pure Ce, the Ce-Sb interdiffusion layers (grey and light grey), and mounting resin (black). The thickness of the total diffusion layer is up to 160 μm. The Ce-Sb layer thickness throughout the interface was not uniform, as largely affected by the amount of Sb powder deposited on the surface. At places where more Sb powder deposited, the total layer was thicker. In the Ce-Sb interdiffusion layers, the light grey region (points 1-4 in Table 2) is comprised of 30-33 at.% Sb, with the remainder being Ce, corresponding to the intermetallic compound Ce_2Sb. The grey region (points 5-7) is comprised of 15-21 at.% Sb, indicating Sb diffused into Ce without a compound formation.

In the right SEM image of Figure 3, from right to left, there are pure Fe, Fe-Sb diffusion layer, and mounting resin (black). The light grey granule-like areas have 55-57 at.% Fe (points 10-12 in Table 2), making the likely phase $Fe_{1.27}Sb$. There are also regions with higher amount of Sb (point 13), possibly due to some $FeSb_2$ being formed, or this could be due to a larger particle of Sb deposited initially that did not fully react.

Accordingly, the Sb-contained binary phases were found in each metal, however, the Ce-Fe-Sb ternary phase was not found. This diffusion couple test was also performed for 120 h (not shown), and again no ternary phase was found. The results were essentially identical in terms of phases formed.

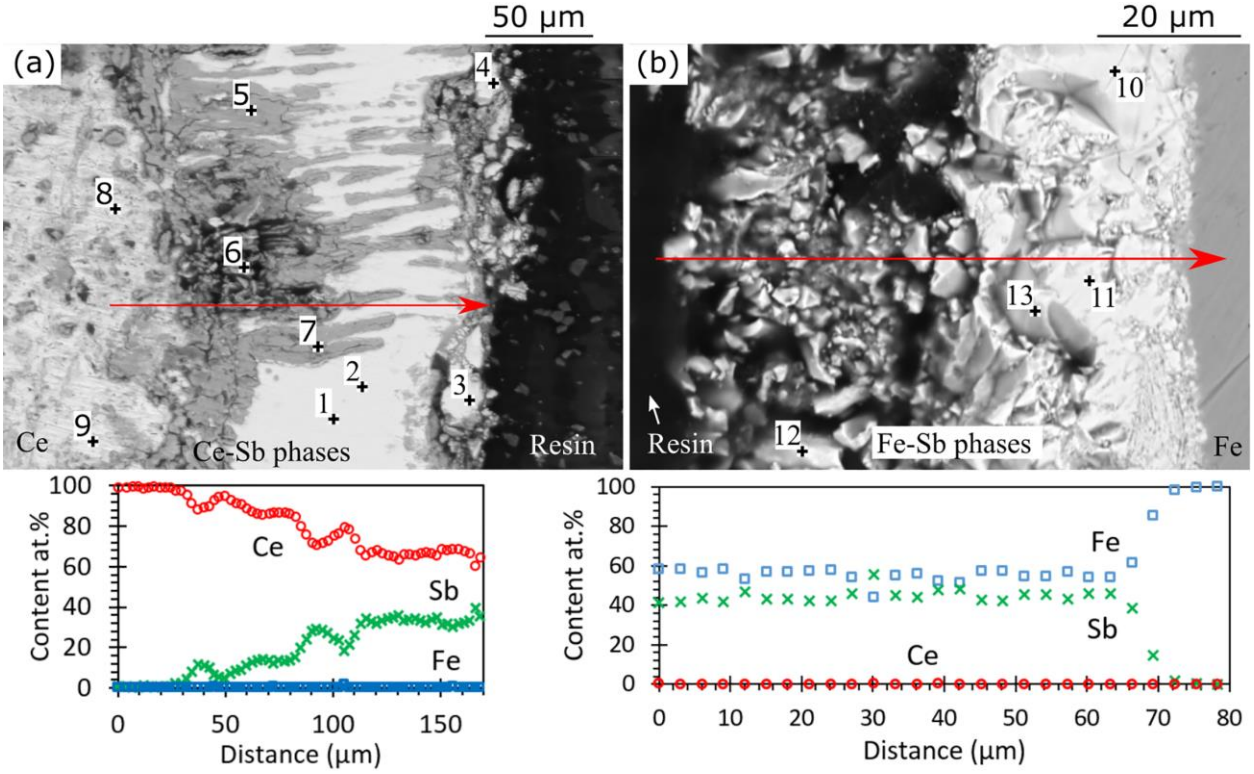

Figure 3. SEM BSE image for the cross section of Ce-Sb-Fe diffusion couple (top) and elemental profile corresponding to the scan line (bottom). Left: Ce disc, right: Fe disc. EDS data are listed in Table 2.

Table 2. EDS data for points shown in Figure 3a (at.%).

	Fe	Sb	Ce
1	0.00	33.15	66.85
2	0.00	30.89	69.11
3	0.00	31.69	68.31
4	0.00	33.10	66.90
5	0.00	18.33	81.67
6	0.00	15.08	84.92
7	0.00	20.74	79.26
8	0.00	0.22	99.78
9	0.00	0.00	100.00
10	55.74	44.26	0.00
11	56.08	43.92	0.00
12	56.74	43.26	0.00
13	49.70	50.30	0.00

The Sb-diffused Ce surface, which contains Ce_2Sb as shown in Figure 3a, was directly coupled with a new Fe disc, and the diffusion couple was run at 853 K for 72 h. This was performed to explore the reactivity between the Ce-Sb compounds and Fe. After heat-treatment, the two discs were separated, behaving the same as the Sb added Ce-Sb-Fe diffusion couple after heat-treatment. Figure 4 shows the cross section SEM images of Ce (Figure 4a) and Fe (Figure 4b). In the Ce cross section, the compositions of the Ce-Sb layer (points 1-5 in Table 3) are the same as observed in Figure 3a, with no Fe obtained in this layer. The Ce-rich phase was found at the bounding surface (point 9), due to Ce diffusing out from the substrate. On the Fe cross section, Figure 4b, a diffusion layer was not formed. An extremely small amount of Ce was adhered on the bounding surface (points 11&12), being from the Ce-rich phase at the bounding surface. The results indicate that the Ce-Sb compounds pre-formed on the bounding surface were very stable and did not react with Fe.

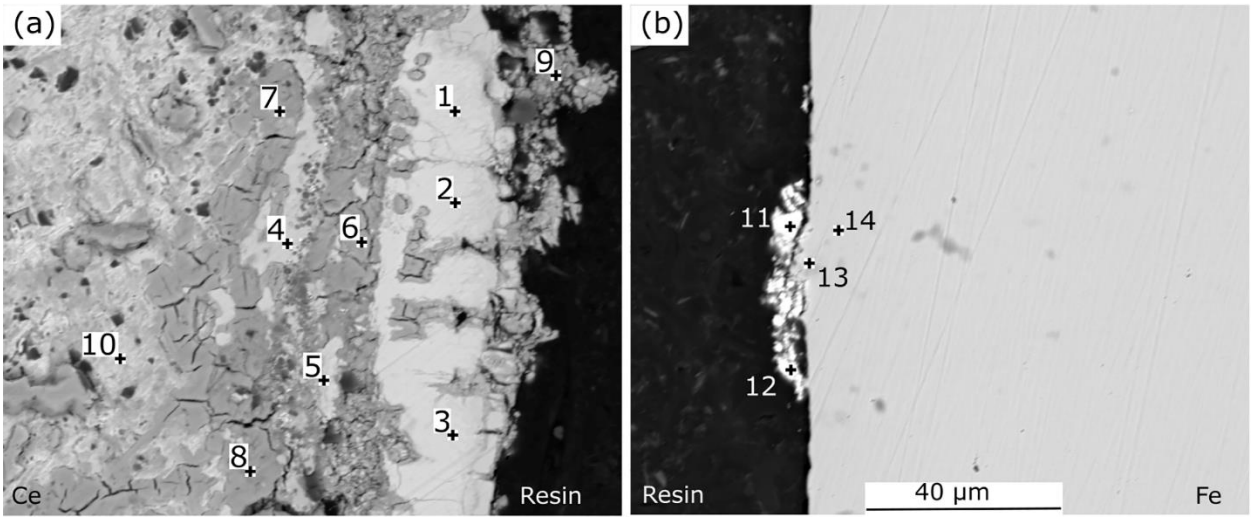

Figure 4. SEM BSE image for the cross section of Sb-diffused Ce disc re-coupled with a new Fe disc. Left: Ce disc, right: Fe disc. EDS data are listed in Table 3.

Table 3. EDS data for points shown in Figure 4 (at.%).

	Fe	Sb	Ce
1	0.00	31.94	68.06
2	0.00	29.17	70.83
3	0.00	31.97	68.03
4	0.00	4.48	95.52
5	0.00	22.82	77.18
6	0.00	0.28	99.72
7	0.00	0.08	99.92
8	1.66	0.15	98.19
9	0.00	6.66	93.34
10	0.00	0.00	100.00
11	2.79	0.00	97.21
12	6.59	0.93	92.48
13	88.74	0.65	10.61
14	99.96	0.00	0.04

The Sb-diffused Fe surface, which has $Fe_{1.27}Sb$ as shown in Figure 3b, was directly coupled with a new Ce disc at 853 K for 72 h. The two discs reacted during the heat-treatment, and did not separate after the test. The cross section SEM image is shown in Figure 5, with EDS data listed in Table 4. From left to right, the phases are pure Fe, $CeFe_2$ (points 1 and 2 in Table 4), Ce_2Sb (points 3-5), Ce (points 6 and 7), and Ce-rich phase with a small amount of Fe and Sb diffused (points 8-10). In the Ce-Fe-Sb system, three ternary compounds $Ce_2Fe_4Sb_5$, $CeFe_{0.6}Sb_2$, and $CeFe_4Sb_{12}$ were found [23]; however, the Ce-rich phase (points 8-10) does not satisfy the composition of a ternary compound, more likely, it is a mixing zone of small amount of Fe and Sb diffused into the Ce

substrate. The result is very interesting since the pre-formed $Fe_{1.27}Sb$ compound disappeared with the formation of Ce_2Sb. Ce separated Sb out of the $Fe_{1.27}Sb$ compound, and then bound Sb to form a new compound. Note that the formation of phase $CeFe_2$ (points 1 and 2) occurred because Ce and Fe directly contacted during the heat-treatment when Sb was separated out from the $Fe_{1.27}Sb$ layer. Again, there was no Ce-Fe-Sb ternary phase observed at the interface.

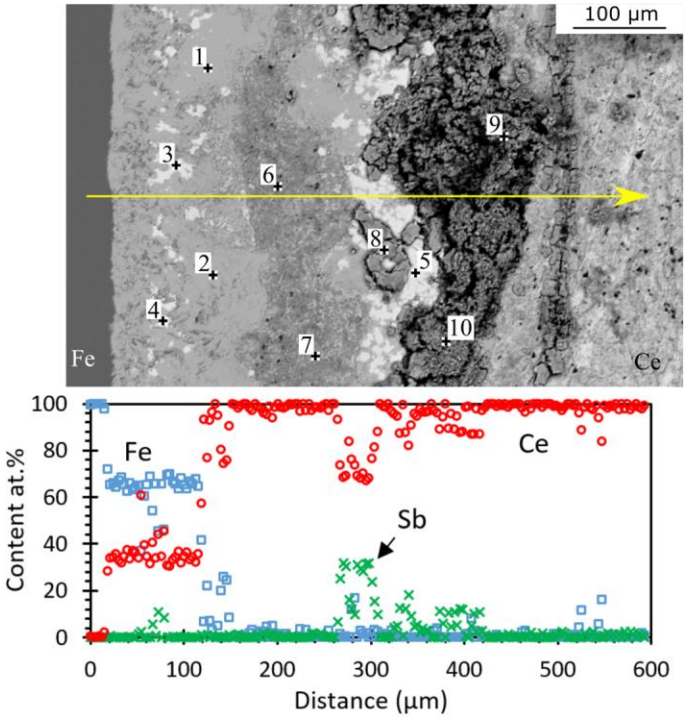

Figure 5. SEM BSE image (top) for the cross section of Sb-diffused Fe disc re-coupled with a new Ce disc. Bottom: elemental profile corresponding to the scan line. EDS data are listed in Table 4.

Table 4. EDS data for points shown in Figure 5 (at.%).

	Fe	Sb	Ce
1	67.51	0.00	32.49
2	67.60	0.10	32.29
3	0.00	31.54	68.46
4	0.37	31.79	67.85
5	0.00	32.11	67.89
6	0.42	0.02	99.56
7	0.00	0.00	100.00
8	1.70	3.02	95.29
9	7.10	6.40	86.49
10	5.92	11.76	82.33

The formation enthalpy of Ce-Sb compounds [12] and Fe-Sb compounds [13] can be used to explain these behaviors. The formation enthalpy of Ce-Sb system is more negative than Fe-Sb system, as shown in Table 5. The more negative value indicates the greater driving force for compound formation and the greater stability.

The present work was performed isothermally out-of-pile. During actual fuel irradiation, the temperature distribution in the fuel may provide higher mobility and driving force for diffusion and migration. Fission damage may also affect the kinetics of Ce-Sb compounds dissolution. Future studies are needed to focus on the effects of temperature gradient and irradiation.

Table 5. Enthalpy of formation (kJ/g-atom) in the systems of Ce-Sb [24] and Fe-Sb [25].

Ce-Sb system (300 K)	Ce_2Sb	Ce_4Sb_3	CeSb	$CeSb_2$
	-102.9	-116.7	-126.4	-90
Fe-Sb system (298 K)	$Fe_{1.27}Sb$	$FeSb_2$		
	-5.1	-11.8		

4. Conclusion

The present work investigated the stability of Ce-Sb compounds when in contact with Fe. It has been found that the addition of Sb changes the Ce-Fe diffusion behavior. Ce and Fe can interdiffuse and form $CeFe_2$ compound. With Sb deposit on the bounding surface, the Ce-Sb and Fe-Sb compounds can form and the Sb acts as a barrier preventing the formation of Ce-Fe compounds. The Ce-Sb compounds are very stable that do not react with Fe. The Fe-Sb compounds, when in contact with Ce, can decompose for the formation of Ce-Sb compounds. The Ce-Sb compounds thereby exhibit a greater thermodynamic stability when in contact with Fe, which is optimal to the metallic fuel with Sb additive. The present work indicates that for a metallic fuel with the additive Sb, the Ce-Sb compounds may be very stable and will not react with Fe, the major cladding constituent. Since the work was done out-of-pile, the in-pile tests are needed to study the kinetics of the Ce-Sb compounds dissolution by fission damage coupled with fission-enhanced diffusion.

Acknowledgement

The authors acknowledge the financial support of U.S. Department of Energy Nuclear Energy University Program [grant number DE-NE0008574].

References

[1] C. Matthews, C. Unal, J. Galloway, D. D. Keiser and S. L. Hayes, Nucl. Technol., vol. 198, pp. 231-259, 2017. http://dx.doi.org/10.1080/00295450.2017.1323535

[2] D. D. Keiser, "Fuel-Cladding Interaction Layers in Irradiated U-Zr and U-Pu-Zr Fuel Elements (ANL-NT-240)," Argonne National Laboratory, Argonne, IL, 2006.

[3] W. J. Carmack, H. M. Chichester, D. L. Porter and D. W. Wootan, J. Nucl. Mater., vol. 473, pp. 167-177, 2016. https://doi.org/10.1016/j.jnucmat.2016.02.019

[4] D. D. Keiser, "The development of fuel cladding chemical interaction zones in irradiated U-Zr and U-Pu-Zr fuel elements with stainless steel cladding," in Nuclear Reactors, Nuclear Fusion, and Fusion Engineering (Editors: A. Aasen and P. Olsson), New York, Nova Science Publishers, Inc., 2009, pp. 163-194.

[5] G. Bozzolo, H. O. Mosca, A. M. Yacout and G. L. Hofman, J. Nucl. Mater., vol. 407, pp. 228-231, 2010. https://doi.org/10.1016/j.jnucmat.2010.10.001

[6] Y. Xie, M. Benson, J. King, R. Mariani and J. Zhang, J. Nucl. Mater., vol. 498, pp. 332-340, 2018. https://doi.org/10.1016/j.jnucmat.2017.10.039

[7] R. D. Mariani, D. L. Porter, T. P. O'Holleran, S. L. Hayes and J. R. Kennedy, J. Nucl. Mater., vol. 419, pp. 263-271, 2011. https://doi.org/10.1016/j.jnucmat.2011.08.036

[8] M. T. Benson, J. A. King, R. D. Mariani and M. C. Marshall, J. Nucl. Mater., vol. 494, pp. 334-341, 2017. https://doi.org/10.1016/j.jnucmat.2017.07.057

[9] Y. S. Kim, T. Wiencek, E. O'Hare, J. Fortner, A. Wright, J. S. Cheon and B. O. Lee, J. Nucl. Mater., vol. 484, pp. 297-306, 2017. https://doi.org/10.1016/j.jnucmat.2016.11.012

[10] X. Su and J.-C. Tedenac, CALPHAD, vol. 30, p. 455–460, 2006. https://doi.org/10.1016/j.calphad.2006.06.003

[11] C. Li, D. Zhu, Y. Zhang, Z. Du, C. Guo, J. Li and J.-C. Tedenac, CALPHAD, vol. 47, pp. 23-34, 2014. https://doi.org/10.1016/j.calphad.2014.05.005

[12] A. Borsese, G. Borzone, D. Mazzone and R. Ferro, J. Less-Common Met., vol. 79, pp. 57-63, 1981. https://doi.org/10.1016/0022-5088(81)90051-5

[13] M. E. Schlesinger, Chem. Rev., vol. 113, pp. 8066-8092, 2013. https://dx.doi.org/10.1021/cr400050e

[14] T. Ogata, M. Kurata, K. Nakamura, A. Itoh and M. Akabori, J. Nucl. Mater., vol. 250, pp. 171-175, 1997. https://doi.org/10.1016/S0022-3115(97)00262-6

[15] J. Delamare, D. Lemarchand and P. Vigier, J. Alloys Compd., vol. 216, pp. 273-280, 1994. https://doi.org/10.1016/0925-8388(94)01271-I

[16] A. A. Kodentsov, G. F. Bastin and F. J. J. van Loo, J. Alloys Compd., vol. 320, pp. 207-217, 2001. https://doi.org/10.1016/S0925-8388(00)01487-0

[17] W. Lo, N. Silva, Y. Wu, R. Winmann-Smith and Y. Yang, J. Nucl. Mater., vol. 458, pp. 264-271, 2015. https://doi.org/10.1016/j.jnucmat.2014.12.035

[18] P. C. Tortorici and M. A. Dayananda, Journal of Nuclear Materials, vol. 204, pp. 165-172, 1993. https://doi.org/10.1016/0022-3115(93)90213-I

[19] G. W. Egeland, R. D. Mariani, T. Hartmann, D. L. Porter, S. L. Hayes and J. R. Kennedy, J. Nucl. Mater., vol. 440, pp. 178-192, 2013. https://doi.org/10.1016/j.jnucmat.2013.04.060

[20] J. M. Harp, D. L. Porter, B. D. Miller, T. L. Trowbridge and W. J. Carmack, J. Nucl. Mater., vol. 494, pp. 227-239, 2017. https://doi.org/10.1016/j.jnucmat.2017.07.040

[21] A. Kodentsov and A. Paul, "Chapter 6 – diffusion couple technique: a research tool in materials science," in Handbook of Solid State Diffusion (A. Paul, S. Divinski, Eds.), 2017, pp. 207-275. https://doi.org/10.1016/B978-0-12-804548-0.00006-2

[22] I. A. Drozdov, Powder Metall. Met. Ceram., vol. 34, pp. 282-287, 1995. https://doi.org/10.1007/BF00560131

[23] J. W. Kaiser and W. Jeitschko, J. Alloys Compd., vol. 291, pp. 66-72, 1999. https://doi.org/10.1016/S0925-8388(99)00252-2

[24] A. Borsese, G. Borzone, D. Mazzone and R. Ferro, vol. 79, no. 1, pp. 57-63, 1981. https://doi.org/10.1016/0022-5088(81)90051-5

[25] D. Boa, S. Hassam, J. Rogez and K. P. Kotchi, J. Alloys Compd., vol. 365, pp. 228-232, 2004. https://doi.org/10.1016/S0925-8388(03)00685-6